

**Time-reversal anomaly and Josephson effect in time-reversal-invariant topological superconductors**Suk Bum Chung,<sup>1,2</sup> Joshua Horowitz,<sup>2</sup> and Xiao-Liang Qi<sup>2</sup><sup>1</sup>*Department of Physics and Astronomy, University of California Los Angeles, Los Angeles, California 90095, USA*<sup>2</sup>*Department of Physics, Stanford University, Stanford, California 94305, USA*

(Received 1 April 2013; revised manuscript received 8 December 2013; published 23 December 2013)

Topological superconductors are gapped superconductors with protected Majorana surface/edge states on the boundary. In this paper, we study the Josephson coupling between time-reversal-invariant topological superconductors and  $s$ -wave superconductors. The Majorana edge/surface states of time-reversal-invariant topological superconductors in all physical dimensions 1, 2, and 3 have a generic topological property which we name the time-reversal anomaly. Due to the time-reversal anomaly, the Josephson coupling prefers a nonzero phase difference between topological and trivial superconductors. The nontrivial Josephson coupling leads to a current-flux relation with a half period in a superconducting quantum interference device geometry, and also a half-period Fraunhofer effect in dimensions higher than 1. We also show that an in-plane magnetic field restores the ordinary Josephson coupling, as a sharp signature that the proposed effect is a consequence of the unique time-reversal property of the topological edge/surface states. Our proposal provides a simple and general approach to experimentally verify whether a time-reversal-invariant superconductor is topological.

DOI: [10.1103/PhysRevB.88.214514](https://doi.org/10.1103/PhysRevB.88.214514)

PACS number(s): 71.10.Pm, 74.50.+r, 75.10.Jm

**I. INTRODUCTION**

In recent years, topological states of matter such as topological insulators (TIs) and topological superconductors (TSCs) have attracted tremendous theoretical and experimental interest.<sup>1–3</sup> The first example of a TSC is the time-reversal-breaking ( $p + ip$ )-wave superconductor of spinless fermions in two dimensions.<sup>4</sup> More recently, an additional class of TSCs was proposed in time-reversal-invariant (TRI) superconductors,<sup>5–7</sup> which have a time-reversal-invariant pairing order parameter in the bulk, and two-dimensional massless Majorana fermions with linear dispersion on the boundary. Candidate materials for TSCs include the <sup>3</sup>He  $B$  phase,<sup>5–8</sup> Cu-doped Bi<sub>2</sub>Se<sub>3</sub>,<sup>9–11</sup> and  $p$ -type TlBiTe<sub>2</sub>.<sup>12</sup> With these candidate materials, a natural question is what type of experiment can distinguish topological superconductors from trivial superconductors. Several experimental signatures have been proposed<sup>10,13–16</sup> but they are either material specific or highly nontrivial to realize.

In this paper, we point out a topological effect that is easy to measure with current experimental techniques and can be used to distinguish TSCs from ordinary SCs in all physical spatial dimensions  $D = 1, 2, 3$ . We consider the Josephson coupling between TSCs and  $s$ -wave superconductors. The regular Josephson coupling in such a junction is very weak due to the different pairing symmetries, but the Majorana surface states induce a nontrivial unconventional Josephson coupling. The most dramatic feature of this Josephson junction is that the lowest-energy state does not occur when the relative phase  $\theta$  between the TSC and the  $s$ -wave superconductor is 0 or  $\pi$ . This is because the surface state is gapless at  $\theta = 0$  or  $\pi$ , protected by time-reversal symmetry, while it generically becomes gapped, and thus saves energy, for  $\theta \neq 0, \pi$ .

The behavior of this topological Josephson coupling depends on whether the system has fermion-number parity conservation. (As we will discuss, this can be controlled by tuning the Josephson frequency.) In a junction with fermion-number parity conservation, the Josephson current has the ordinary frequency, but has a phase shift depending

on the fermion-number parity (i.e., fermion number mod 2) of the junction. In particular, at  $\theta = 0$  or  $\pi$  there is a finite supercurrent, the sign of which depends on the fermion-number parity. This is a direct measurement of the following generic feature of the TSC surface states:<sup>7</sup>

$$\mathcal{T}^{-1}(-1)^{N_F}\mathcal{T} = -(-1)^{N_F}. \quad (1)$$

Here  $N_F$  is the fermion number of the system. Since all electrons are paired in the superconducting state except for the zero modes, the fermion-number parity  $(-1)^{N_F} = i\gamma_{0\uparrow}\gamma_{0\downarrow}$  is determined by the Majorana zero modes  $\gamma_{0\uparrow, \downarrow}$ . Equation (1) then directly follows from the time-reversal transformation  $\mathcal{T}^{-1}\gamma_{0\uparrow}\mathcal{T} = \gamma_{0\downarrow}$ ,  $\mathcal{T}^{-1}\gamma_{0\downarrow}\mathcal{T} = -\gamma_{0\uparrow}$ . Since fermion-number parity should be preserved microscopically by time-reversal transformation, the anticommutation between time reversal and fermion-number parity given by Eq. (1) is forbidden in a closed TRI superconductor. However, such violation of fermion parity conservation is allowed to occur on the surface of a TRI TSC, while the symmetry is still preserved in the whole system with an even number of independent surfaces. This is then an instance where a symmetry present on the classical level is broken on the surface of a topological phase due to the topological properties of the bulk state. In other words, the anticommutation relation (1) can be regarded as a quantum anomaly of the TSC surface state. This is a direct analog of the parity anomaly<sup>17,18</sup> that occurs at the surface of a three-dimensional (3D) TI with TR-symmetry (TRS) breaking.<sup>14,19</sup> In the case of a TI surface state, the TR symmetry changes the surface Hall conductance by an odd integer in units of  $\frac{e^2}{h}$ , so that the Hall conductance of the surface state in a TR-breaking insulating state is always a half-odd-integer in the same units. The anomalous relation between TR transformation and fermion-number parity given by Eq. (1) is a superconducting analog of the half-integer Hall conductance. We name this property of the surface state the *time-reversal anomaly*. As a direct consequence of the time-reversal anomaly, we show that a superconducting quantum interference device (SQUID) shown in Fig. 1(a) has

maximal critical current at the flux  $\Phi = hc/4e$  for an odd number of electrons in the system and at  $\Phi = 0$  for an even number of electrons.

When the fermion number in the Josephson junction is fluctuating due to impurity scattering, the behavior of the junction is still qualitatively different from that of an ordinary Josephson junction. The Josephson current has a doubled frequency due to the anomalous energy-phase relation. This can be experimentally detected in the behavior of the SQUID and for the  $D = 2, 3$  case in the Fraunhofer effect. In particular, we show that an in-plane magnetic field comparable with the pairing gap at the Josephson junction can drive the junction back to a normal one, which provides a clear signature that time-reversal symmetry plays an essential role in the topological Josephson effect. It should be clarified that the topological Josephson effect discussed in this work is qualitatively different from the fractional Josephson effect discussed in Refs. 20 and 21, which applies to different physical systems and also has different phenomenology.

## II. MODEL HAMILTONIAN

Although our proposal applies to a generic TSC, for the concreteness of our discussion we would like to start by defining some model systems for TRI TSCs. TSCs in  $D = 1, 2, 3$  can all be realized in the following lattice Bogoliubov–de Gennes (BdG) Hamiltonian:

$$H_p = -\mu \sum_{rs} c_{rs}^\dagger c_{rs} - t \sum_{i=1}^D \sum_{rs} (c_{\mathbf{r}+\hat{\mathbf{e}}_i, s}^\dagger c_{rs} + \text{H.c.}) \\ + \sum_{i=1}^D \sum_{rs'} [\Delta(-\hat{\mathbf{e}}_i \cdot \boldsymbol{\sigma} \sigma_z)_{ss'} c_{\mathbf{r}+\hat{\mathbf{e}}_i, s}^\dagger c_{rs'}^\dagger + \text{H.c.}], \quad (2)$$

with  $-2Dt < \mu < -2(D-2)t$ . In  $D = 2$  (3), the model is defined on a square (cubic) lattice, so  $\mathbf{r}$  denotes the lattice sites and the  $\hat{\mathbf{e}}_i$ 's ( $i = 1, 2, \dots, D$ ) are the orthogonal unit vectors.  $\boldsymbol{\sigma} = (\sigma_x, \sigma_y, \sigma_z)$  denotes the Pauli matrices, and  $s = \uparrow, \downarrow$  the electron spin index.

## III. JOSEPHSON EFFECT IN 1D TSC

We start from the 1D TSC, which gives us the clearest example of how the Josephson coupling between the TRI TSC and the  $s$ -wave SC arises from time-reversal-symmetry breaking. The candidate materials include a class of quasi-1D organic superconductors<sup>22</sup> and LiMoO.<sup>23</sup> 1D is distinct from 2D and 3D in the sense that there is a finite gap separating the Majorana zero modes from other quasiparticle excitations. As will be discussed below, such a gap makes it possible to probe the ‘‘TR anomaly’’ of Eq. (1), i.e., the fact that time reversal changes the fermion-number parity of the Majorana zero modes.

The 1D Josephson junction we consider here is described by the Hamiltonian  $H = H_p + H_s + H_1$ , with  $H_p$  the Hamiltonian of a 1D TRI TSC chain given by Eq. (2) with  $D = 1$ ,  $H_s$  that of an  $s$ -wave SC chain, and  $H_1$  a spin-conserving hopping between the first site of the TSC chain and the last site (labeled  $m$ ) of the  $s$ -wave chain:

$$H_1 = - \sum_{\sigma} [(\delta t) c_{1\sigma}^\dagger f_{m\sigma} + \text{H.c.}], \quad (3)$$

In the rest of our paper, we will focus on weak hopping, e.g.,  $|\delta t/t| \ll 1$ , although our numerical methods also apply to the  $|\delta t/t| \sim 1$  case analogous to Ref. 24.

For small coupling  $\delta t$  we can study the Josephson coupling by perturbation theory. Since the TSC and the  $s$ -wave SC are both gapped, the main effect of a small  $\delta t$  is to couple the Majorana zero modes at the boundary of the TSC. We start from the special case  $\mu = 0, \Delta = t$  for the TSC, in which case the TSC Hamiltonian can be written as  $H_p = -t \sum_{n\sigma} (c_{n+1,\sigma} + c_{n+1,\sigma}^\dagger)(c_{n,\sigma} - c_{n,\sigma}^\dagger)$ ,<sup>20</sup> and the Majorana zero modes are completely localized at the boundary site:  $\gamma_{0\sigma} = c_{1\sigma} + c_{1\sigma}^\dagger$ . Therefore the interchain hopping  $H_1$  can be written as  $H_1 = - \sum_{\sigma} [ \frac{\delta t}{2} \{ \gamma_{0\sigma} - (c_{1,\sigma} - c_{1,\sigma}^\dagger) \} f_{m\sigma} + \text{H.c.}]$ . Only the zero mode contributes to the lowest-order perturbation, which gives the effective Hamiltonian

$$H_{\text{eff}} = J(i\gamma_{0\uparrow}\gamma_{0\downarrow}) \sin \phi, \quad (4) \\ iJ = (\delta t)^2 \int dt \langle T f_{m\uparrow}(t) f_{m\downarrow}(0) \rangle_{\Delta'=i|\Delta'|},$$

where  $\Delta'$  is the pairing gap of the  $s$ -wave chain and  $\phi$  its phase; our gauge is set to give us a real  $\delta t$  and  $\langle T \dots \rangle$  denotes the time-ordered expectation value. This effective Hamiltonian has time-reversal symmetry, both  $\sin \phi$  and  $i\gamma_{0\uparrow}\gamma_{0\downarrow}$  being time-reversal odd. This means that if the Majorana zero-mode pair does not form a Kramers doublet,<sup>25,26</sup> the  $\phi$  dependence of the effective Hamiltonian will be different. It remains valid for generic parameters  $\mu, \Delta$  even though the Majorana zero mode  $\gamma_{0\sigma}$  is not completely localized at one site.

The effective Hamiltonian Eq. (4) can give us a nonzero Josephson current for the relative phase preserving time-reversal symmetry:  $\phi = 0, \pi$ . In a clean system, the local fermion-number parity  $i\gamma_{0\uparrow}\gamma_{0\downarrow}$  is conserved at  $T = 0$ . In a realistic system, it may change, e.g., by a fermion leaking from the zero modes to some impurity sites, at a rate we denote as  $1/\tau$ . However, if the dc bias voltage  $V$  of the junction is large enough so that  $\omega_J \equiv 2eV/\hbar \gg 1/\tau$ ,  $i\gamma_{0\uparrow}\gamma_{0\downarrow}$  is quasiconserved, i.e., it will not change in many Josephson periods. In this fast limit, our Josephson coupling should be taken to be  $E_{\pm} = \pm J \sin \phi$  for  $i\gamma_{0\uparrow}\gamma_{0\downarrow} = \pm 1$ , respectively, giving us the Josephson current of  $I(\phi = 0, \pi) = \pm I_c$  where  $I_c \equiv 2eJ/\hbar$ . A nonvanishing Josephson current usually occurs in a TRS-breaking junction.<sup>27,28</sup> Since our system is TR invariant, the finite  $I_c$  is a direct manifestation that the  $i\gamma_{0\uparrow}\gamma_{0\downarrow}$  eigenstates break TR symmetry.

In contrast, in the slow limit  $\omega_J \tau/\pi \sim 1$  we have a  $\pi$ -periodic Josephson oscillation with discontinuities of  $I(\phi)$  at  $\phi = 0, \pi$ . Note that the system can stay at the ground-state energy  $E_G = -J|\sin \phi|$  of the effective Hamiltonian Eq. (4) if  $i\gamma_{0\uparrow}\gamma_{0\downarrow}$  switches at the rate of  $\omega_J/\pi$ . Therefore in this slow limit, this parity switching is always likely at  $\phi = 0, \pi$ , giving us the current-phase relation of  $I(\phi) = I_c \frac{d}{d\phi} (-|\sin \phi|) = -I_c \frac{|\sin \phi|}{\sin \phi} \cos \phi$ .

To physically observe this behavior of the Josephson junction, we now consider a dc SQUID consisting of two such Josephson junctions with flux  $\Phi$  threading through, as shown in Fig. 1(a). Each of the two junctions has a Kramers doublet of Majorana zero modes  $\gamma_{0\sigma}$  and  $\gamma'_{0\sigma}$ , where, for  $\mu = 0$  and  $\Delta = t$ ,  $\gamma'_{0\sigma} = -i(c_{N\sigma} - c_{N\sigma}^\dagger)$ . Therefore, the

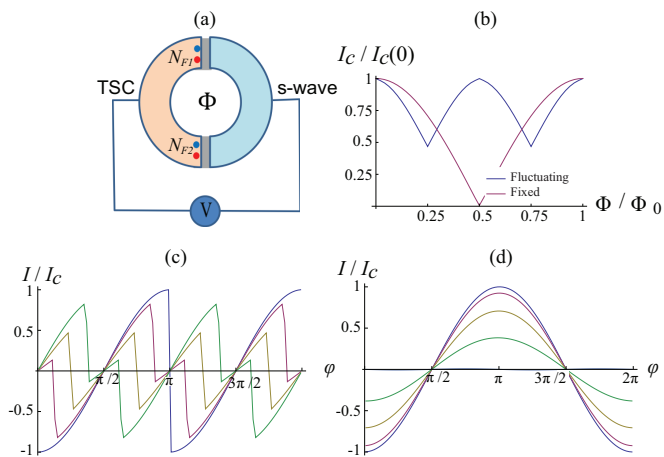


FIG. 1. (Color online) (a) Schematic picture of a dc voltage-biased SQUID. (b) Dependence of the current oscillation amplitude on the flux  $\Phi$ . (c),(d) Numerical calculation of the dc SQUID  $I/I_c$  as a function of  $\phi$  for the flux of  $\Phi/\Phi_0 = 0, 1/8, 1/4, 3/8, 1/2$  in blue, purple, brown, green, and black respectively; (c) is for the slow limit and (d) for the fast limit with odd local fermion parity.

effective Hamiltonian of this SQUID is

$$H_{\text{eff}} = -J[N_{F1} \sin(\phi - \pi \Phi/\Phi_0) + N_{F2} \sin(\phi + \pi \Phi/\Phi_0)], \quad (5)$$

where  $\Phi_0 = h/2e$  is the quantum flux and  $N_{F1} = i\gamma_{0\uparrow}\gamma_{0\downarrow}$ ,  $N_{F2} = -i\gamma'_{0\uparrow}\gamma'_{0\downarrow}$  are the local fermion-number parities of the two junctions. In the slow limit the system stays at the lowest-energy state with energy  $E_J = -J[|\sin(\phi - \pi \Phi/\Phi_0)| + |\sin(\phi + \pi \Phi/\Phi_0)|]$ , so that the current-flux relation is

$$\frac{I}{I_c} = -\sum_{s=\pm} \frac{\sin\left(\phi + s\pi \frac{\Phi}{\Phi_0}\right)}{|\sin\left(\phi + s\pi \frac{\Phi}{\Phi_0}\right)|} \cos\left(\phi + s\pi \frac{\Phi}{\Phi_0}\right). \quad (6)$$

As shown on Fig. 1(c),  $I(\phi)$  has four discontinuities per  $2\pi$  period due to the fluctuations of  $N_{F1}$  and  $N_{F2}$  except at  $\Phi = n\Phi_0$  and  $\Phi = (n + 1/2)\Phi_0$ , where  $N_{F1}$  and  $N_{F2}$  fluctuate together.

Due to the TR anomaly, when the fermion parity is conserved, this dc SQUID behaves like a normal SQUID for an even number of electrons and a  $\pi$  SQUID for an odd number of electrons; this implies that the SQUID behavior is determined hysteretically. When the local fermion parities do not fluctuate, we have four possible current-phase relations determined by the eigenvalues of  $N_{F1}$  and  $N_{F2}$ ,

$$I = \begin{cases} -2N_{F1}I_c \cos(\pi \Phi/\Phi_0) \cos \phi, & N_{F1}N_{F2} = +1, \\ -2N_{F1}I_c \sin(\pi \Phi/\Phi_0) \sin \phi, & N_{F1}N_{F2} = -1, \end{cases} \quad (7)$$

which gives us a normal SQUID for even total fermion parity  $N_{F1}N_{F2} = +1$  and a  $\pi$  SQUID for odd total fermion parity  $N_{F1}N_{F2} = -1$ . In the latter case, the SQUID at zero flux has a spontaneous circulating current,<sup>29</sup> as a clear signature of spontaneous time-reversal-symmetry breaking. We see from Fig. 1(c) that, even in the slow limit, the SQUID is in the  $N_{F1}N_{F2} = +1$  eigenstate at  $\Phi = n\Phi_0$  and the  $N_{F1}N_{F2} = -1$  eigenstate at  $\Phi = (n + 1/2)\Phi_0$ . Therefore we can obtain the

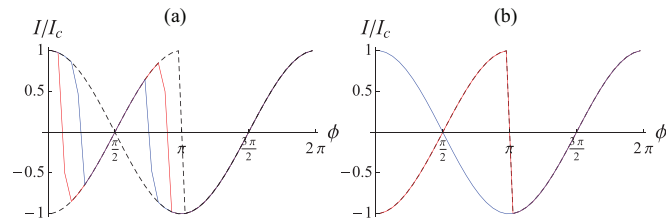


FIG. 2. (Color online) The Zeeman field effect on the Josephson current in the slow limit for  $\delta t/\Delta = 0.2$ . (a) The Zeeman field is applied along the junction with the magnitude of  $g\mu_B h/\Delta = 0$  (black dashed), 0.005 (blue), 0.01 (red), and 0.02 (brown). (b) The Zeeman field of magnitude  $g\mu_B h/\Delta = 0.02$  applied along the junction (red) and perpendicular to the junction (blue). While the field along the junction changes the location of the discontinuity and eventually removes it altogether, the field perpendicular to the junction has negligible effects.

$\pi$  SQUID by ramping up  $\omega_J$  from slow to fast while the flux is fixed at  $\Phi = \Phi_0/2$ , and the normal SQUID by going through the same process at  $\Phi = 0$ . We note that periodicity change controlled by the Josephson frequency has also been proposed<sup>30</sup> in topological insulator/superconductor systems,<sup>31</sup> but the physical mechanism studied there is different, and the periodicity change there is between  $4\pi$  and  $2\pi$ .

The TR anomaly can also be revealed through the effect of the Zeeman field. The Zeeman field breaks TRI and provides an alternative channel for gapping out the Majorana zero modes. To the leading order, our effective Hamiltonian of a single junction is modified to

$$H_{\text{eff}} = (i\gamma_{0\uparrow}\gamma_{0\downarrow})(J \sin \phi + g\mu_B \mathbf{h} \cdot \hat{\mathbf{n}}), \quad (8)$$

where  $g$  is the normal-state  $g$  factor of the TRI TSC,  $\mu_B$  the Bohr magneton,  $\mathbf{h}$  the effective Zeeman field, and  $\hat{\mathbf{n}}$  a unit vector along the junction.<sup>8,32</sup> As in Eq. (4), this form of the Zeeman field dependence requires that the Majorana zero-mode pair form a Kramers doublet. We can see that once  $\mathbf{h} \cdot \hat{\mathbf{n}} > J/(g\mu_B)$ , there is no level crossing between the even- and odd-parity states, giving us a conventional Josephson junction. The numerical calculation shown in Fig. 2 confirms both the sensitivity to the Zeeman field direction and the absence of level crossings at sufficiently strong field. This Zeeman field effect is due to both spin accumulation<sup>28,33</sup> and the Zeeman-field-induced  $s$ -wave pairing on the TRI TSC boundary. We will show that analogous effects exist also in higher dimensions.

#### IV. GENERALIZATION TO HIGHER DIMENSIONS

In higher dimensions, the TR anomaly leads to a Zeeman-field-induced period-doubling in the  $s$ -wave/TRI TSC Josephson junction. As in 1D, this tunneling gaps the boundary state for the relative phase  $\phi \neq 0, \pi$ . However, as the boundary state of a TRI TSC has a continuous spectrum, we are always in the slow limit  $\omega_J \tau \ll 1$ . Just as in 1D, the Josephson coupling between a TSC and an  $s$ -wave SC can be described by the coupling Hamiltonian  $H_1 = -\sum_{n=1}^{N_y} \sum_{\sigma} [(\delta t)c_{\sigma}^{\dagger}(1, n)f_{\sigma}(m, n) + \text{H.c.}]$  ( $n = 1, 2, \dots, N_y$  labels the boundary sites).

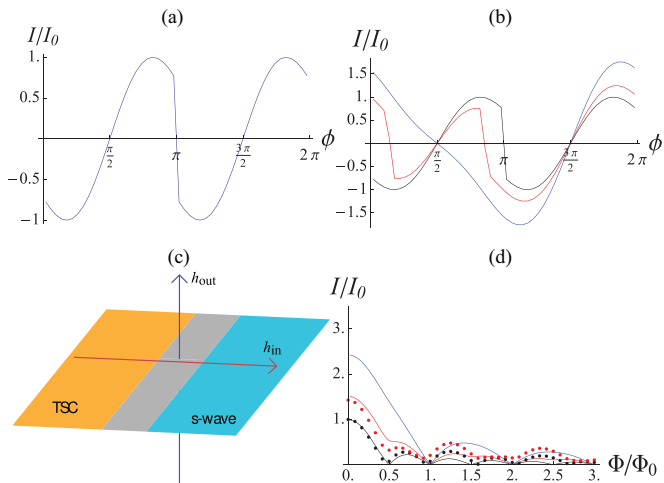


FIG. 3. (Color online) We have set  $|\delta t|/\Delta = 0.7$ . (a) Numerical results for the current-phase relation  $I(\phi)$ . (b) Numerical results for  $I(\phi)$  with the Zeeman field  $\tilde{h}/|\Delta| = 0$  (black), 0.02 (red), and 0.06 (blue) along the junction. (c) The scheme for the Fraunhofer diffraction experiment.  $h_{\text{out}}$  gives us the flux  $\Phi$  through the junction,  $h_{\text{in}}$  gives rise to Eq. (11). (d) The Fraunhofer diffraction pattern with the Zeeman field  $\tilde{h}/|\Delta| = 0$  (black), 0.02 (red), and 0.06 (blue) along the junction; the filled curves are calculated from the current-phase relation Eq. (12) and the dots from the numerical calculation.

We will now show that we have a  $\pi$ -periodic Josephson coupling in the higher dimensions. In the weak-tunneling limit, the boundary-state gap can be calculated by perturbation theory exactly analogously to that of the 1D case. Here we omit this derivation and directly write down the effective edge theory induced by the tunneling:

$$H_{\text{eff}} = \sum_k [vk(\gamma_{-k\uparrow}\gamma_{k\uparrow} - \gamma_{-k\downarrow}\gamma_{k\downarrow}) + i(M \sin \phi)\gamma_{-k\downarrow}\gamma_{k\uparrow}] \quad (9)$$

for the 1D Majorana edge state of a 2D TSC. As required by TRS, the mass term is proportional to  $\sin \phi$  and roughly the same as in 1D Josephson coupling. The 2D Josephson energy is determined by the change in the ground-state energy of the effective model Eq. (9) due to the nonzero mass  $M \sin \phi$ :

$$E_J(\phi) = \frac{1}{2} \sum_k \left[ -\sqrt{v^2k^2 + M^2 \sin^2 \phi} + v|k| \right]. \quad (10)$$

In the thermodynamic limit the sum becomes an integral and we obtain the energy and current-phase relation

$$E_J(\phi) = -\frac{\Phi_0 I_c}{2\pi} \left[ 1 + \ln \frac{4|\Delta|^2}{M^2 \sin^2 \phi} \right] \sin^2 \phi, \quad (11)$$

$$I(\phi) = -I_c \left[ \ln \frac{4|\Delta|^2}{M^2 \sin^2 \phi} \right] \sin 2\phi,$$

where  $I_c \propto M^2$ . As the Josephson energy Eq. (10) depends only on the mass term squared, we have  $I(\phi + \pi) = I(\phi)$  for the Josephson current, and this is confirmed in the numerical calculation plotted in Fig. 3(a). The same holds for the 3D TSC/*s*-wave junction; there Eq. (9) is also applicable and gives us  $I(\phi) = I_c \sin 2\phi$ .

The in-plane Zeeman field can restore the  $2\pi$  periodicity. Analogously to Eq. (8), the Zeeman effect leads to an additional contribution to the gap of the edge state in the effective Hamiltonian Eq. (9):

$$H_Z = \sum_k i\gamma_{-k\downarrow}\gamma_{k\uparrow}g\mu_B\mathbf{h} \cdot \hat{\mathbf{n}} \quad (12)$$

with  $\hat{\mathbf{n}}$  the edge normal vector. With this modification, the Josephson coupling is  $2\pi$  periodic, with the current-phase relation of

$$I(\phi) = -I_c \left[ \ln \frac{4|\Delta|^2/M^2}{(\sin \phi + \tilde{h}/M)^2} \right] \left( \sin 2\phi + \frac{2\tilde{h}}{M} \cos \phi \right), \quad (13)$$

where  $\tilde{h} \equiv g\mu_B\mathbf{h} \cdot \hat{\mathbf{n}}$ . We see from this formula that for  $|\tilde{h}| \gg |M|$  our Josephson coupling becomes essentially conventional, with the effective critical current nearly proportional to the in-plane field. Given  $|M| \propto (\delta t)^2$ , this crossover occurs in the  $|\tilde{h}| \ll \delta t$  regime, which is confirmed by the numerical calculations shown in Fig. 3(b). The underlying reason is that the Zeeman energy term of Eq. (11) induces *s*-wave pairing. As it also occurs in 3D, this crossover provides a sharp experimental signature of the TSC.

The in-plane Zeeman field can also completely alter the Fraunhofer diffraction in a single Josephson junction. When the magnetic field is perpendicular, the Fraunhofer diffraction pattern for 2D has zeros at both  $\Phi = n\Phi_0$  and  $\Phi = (n + 1/2)\Phi_0$ , since the 2D Josephson current of Eq. (10) has only even harmonics. However, if one measures the Fraunhofer pattern in a canted magnetic field as shown in Fig. 3(c), the critical currents at  $\Phi = (n + 1/2)\Phi_0$  are nonzero as shown in Fig. 3(d), as the current-phase relation, now given by Eq. (12), has nonzero odd harmonics.

## V. EFFECT OF CONVENTIONAL JOSEPHSON COUPLING

The Josephson coupling will be dominated by our topological contribution as long as the spin-orbit-coupled hopping across the junction,  $H_{\text{SOC}} = \sum_{\mathbf{R}} \sum_{\sigma} [\lambda \sigma c_{\mathbf{R}\sigma}^\dagger f_{\mathbf{R}+\hat{\mathbf{n}},\sigma} + \text{H.c.}]$  (the  $\mathbf{R}$ 's are the interface lattice sites and  $\hat{\mathbf{n}}$  the interface normal), which can give rise to the regular  $\sin \phi$  term in the Josephson current  $I(\phi)$ , is weak enough. This leads to the conditions

$$\frac{|\lambda|}{|\delta t|} \ll \frac{|t|}{|\Delta|}$$

for  $D = 1$  and

$$\frac{|\lambda|}{|\delta t|} \ll \frac{|\delta t|^2}{|\Delta|^2}$$

for  $D = 2, 3$  (see Appendix B for the derivation). Lastly we note that it is possible to experimentally rule out the possibility of our effects coming from Kondo impurities in the junction if we do not see the resonant transparency of the junction at a temperature above the critical temperatures of both superconductors.<sup>34</sup>

## ACKNOWLEDGMENTS

It is our pleasure to thank Mac Beasley, Srinivas Raghu, and Shou-Cheng Zhang for sharing their insights with us. This



work is supported by the Department of Energy, Office of Basic Energy Sciences, Division of Materials Sciences and Engineering, under Contract No. DE-AC02-76SF00515.

### APPENDIX A: MODELS OF TSCS IN $D = 1, 2$

Here we present the explicit form of the Hamiltonian Eq. (2) for  $D = 1$  and  $D = 2$ . For our numerical calculation for  $D = 1$  in Figs. 1 and 2, the BdG Hamiltonians for our two superconducting chains are

$$H_p = -\mu \sum_{rs} c_{rs}^\dagger c_{rs} - t \sum_{rs} (c_{r+\hat{x}s}^\dagger c_{rs} + \text{H.c.}) + \sum_{rs} (\Delta c_{r+\hat{x}s}^\dagger c_{rs}^\dagger + \text{H.c.}), \quad (\text{A1})$$

for the TRI TSC and

$$H_s = -\mu' \sum_{r's} f_{r's}^\dagger f_{r's} - t' \sum_{r's} (f_{r'+\hat{x}s}^\dagger f_{r's} + \text{H.c.}) + \sum_{r'} (\Delta' f_{r'\uparrow}^\dagger f_{r'\downarrow}^\dagger + \text{H.c.}) \quad (\text{A2})$$

for the  $s$ -wave chain; note that Eq. (14) can be obtained from the  $D = 1$  case of Eq. (2) by applying a  $-\pi/2$  spin rotation around the  $z$  axis. We have set  $|t| = |t'| = |\Delta| = |\Delta'|$ ,  $\mu_s = \mu_p = 0$ , and  $|\delta t/t| = 0.2$ , and both chains consisted of 100 lattice sites. For the numerical calculation in Fig. 2, we add the Zeeman field term

$$H_Z = -g\mu_B \sum_{ss'} (\mathbf{h} \cdot \boldsymbol{\sigma})_{ss'} \left[ \sum_r c_{rs}^\dagger c_{rs'} + \sum_{r'} f_{r's}^\dagger f_{r's'} \right]. \quad (\text{A3})$$

For the  $D = 2$  numerical calculation in Fig. 3, we used for the TRI TSC the BdG Hamiltonian

$$H_p = -\mu \sum_{rs} c_{rs}^\dagger c_{rs} - t \sum_{\hat{e}=\hat{x},\hat{y}} \sum_{rs} (c_{r+\hat{e}s}^\dagger c_{rs} + \text{H.c.}) + \Delta \sum_{rs} [(c_{r+\hat{x}s}^\dagger c_{rs}^\dagger - i s c_{r+\hat{y}s}^\dagger c_{rs}^\dagger) + \text{H.c.}], \quad (\text{A4})$$

which can be obtained, just as in  $D = 1$ , by applying a  $-\pi/2$  spin rotation around the  $z$  axis. This BdG Hamiltonian gives us  $p_x + ip_y$  pairing between spin-up electrons and  $p_x - ip_y$  pairing between spin-down electrons. The  $s$ -wave SC on a square lattice has the Hamiltonian

$$H_s = -\mu' \sum_{r's} f_{r's}^\dagger f_{r's} - t' \sum_{r's} \sum_{\hat{e}=\hat{x},\hat{y}} (f_{r'+\hat{e}s}^\dagger f_{r's} + \text{H.c.}) + \sum_{r'} (\Delta' f_{r'\uparrow}^\dagger f_{r'\downarrow}^\dagger + \text{H.c.}) \quad (\text{A5})$$

The parameters we used were  $|\Delta| = |\Delta'|$ ,  $|t/\Delta| = |t'/\Delta'| = 3$ ,  $\mu/|\Delta| = \mu'/|\Delta'| = -2$ , and  $|\delta t/\Delta| = 0.7$ . We find that these parameters open up an edge-state gap of  $M/|\Delta| = 0.016$  at  $\phi = \pi/2$ ; the fact that this deviates within an order of magnitude from the crossover value of  $\tilde{h}$  indicated by Fig. 3(b) is because Eq. (13) assumes that the dispersion of the edge state is linear and that the mass term is  $k$  independent, neither of which is strictly true. To obtain the result shown

in Figs. 3(a) and 3(b), we have set our superconductors on lattices of 100 sites along the junction (the  $y$  direction) and 30 sites perpendicular to the junction (the  $x$  direction), and imposed a periodic boundary condition in the  $y$  direction. For the numerical calculation in Fig. 3(d), we have 10 lattice sites along the  $y$  direction (without a periodic boundary condition) and 12 sites along the  $x$  direction; in addition the perpendicular flux  $\Phi$  modifies the hopping between the two superconductors:

$$H_1 = - \sum_{n=1}^{N_y} \sum_{\sigma} [(\delta t) e^{i(2n-N_y-1)\Phi/4\Phi_0} c_{\sigma}^\dagger(1,n) f_{\sigma}(m,n) + \text{H.c.}]. \quad (\text{A6})$$

For the analytical calculation in Fig. 3(d), we used Eq. (13) with  $M = 0.02/\sin(4\pi/25)$ , which is the value we infer from the numerical results in Fig. 3(b).

### APPENDIX B: ADDITIONAL CONTRIBUTIONS FROM THE ORDINARY JOSEPHSON EFFECT

Within our assumption of weak hopping between the two superconductors, the bulk-to-bulk contribution in  $D = 1$  is negligible compared to the contribution of the Majorana zero modes:

$$J = -i(\delta t)^2 \int dt \langle T f_{m\uparrow}(t) f_{m\downarrow}(0) \rangle_{\Delta'=i|\Delta|} = -(\delta t)^2 \frac{1}{N} \sum_k F'(\omega=0, k)_{\Delta'=i|\Delta|} = (\delta t)^2 \int \frac{2d\xi'}{\hbar v_F'} \frac{a'}{2\pi} \frac{1}{2} \frac{|\Delta'|}{\xi'^2 + |\Delta'|^2} = \frac{(\delta t)^2}{4t' \sin k'_F a'}, \quad (\text{B1})$$

where  $k'_F$  is obtained from  $\mu' = 2t' \cos k'_F a'$ . The bulk-to-bulk Josephson coupling can come only from tunneling Cooper pairs between two superconductors. Our numerical calculation of the Josephson coupling is based on an exact diagonalization of  $H_s + H_p + H_1$  for different values of  $\phi$  and thus already includes this bulk-to-bulk contribution for the case where spin is conserved at the junction, and we can see that the bulk contribution is negligible. This is because the bulk-to-bulk coupling is nonzero only at the fourth-order expansion of the parametrically small  $\delta t$ , as the coupling between the spin-triplet TSC and the  $s$ -wave superconductor, which is spin singlet, requires tunneling of one spin-up–spin-up pair and one spin-down–spin-down pair. A nonzero bulk-to-bulk contribution from tunneling of a single Cooper pair requires a nonzero spin flip at the junction, which means including the term

$$H_{\text{SOC}} = \sum_{\sigma=\pm} (\lambda \sigma c_{1\sigma}^\dagger f_{m\sigma} + \text{H.c.}); \quad (\text{B2})$$

however, even after including  $H_{\text{SOC}}$ , we find that the bulk-to-bulk contribution remains very small. With  $H_{\text{SOC}}$ , it is possible for a like-spin pair from the TSC to now tunnel to the  $s$ -wave superconductor as a spin-singlet pair, and hence there will be an ordinary Josephson coupling that contributes a  $\sin \phi$  term

to  $I(\phi)$ . But the strength of this Josephson coupling,

$$\begin{aligned}\tilde{J}_{\text{bulk}} &= 2 \frac{(\delta t)\lambda}{N^2} \sum_{k,k'} \sum_{\sigma=\pm} \frac{\sigma \langle c_{\sigma}^{\dagger}(k) f_{\bar{\sigma}}(k') c_{\sigma}^{\dagger}(-k) f_{\sigma}(-k') \rangle_{\Delta'=|\Delta|}}{E_p(k) + E_s(k')} \\ &= \frac{(\delta t)\lambda}{N^2} \sum_{k,k'} \frac{|\Delta||\Delta'|}{E_p(k)E_s(k')[E_p(k) + E_s(k')]} \\ &= \frac{(\delta t)\lambda|\Delta||\Delta'|}{4\pi^2 t t' |\sin k_F a \sin k'_F a'|} \int \frac{d\xi d\xi'}{E_p E_s} \frac{1}{E_p + E_s}, \quad (\text{B3})\end{aligned}$$

where  $E_p^2 = \xi^2 + |\Delta|^2$  and  $E_s^2 = \xi'^2 + |\Delta'|^2$  (for this calculation we ignored the breaking of translational symmetry at the junction) are much smaller than the Majorana zero-mode contribution

$$\tilde{J}_{\text{bulk}}/J \sim \frac{\lambda}{(\delta t)} \frac{|\Delta|}{t}; \quad (\text{B4})$$

this is because we physically expect the spin-flip tunneling to be smaller than the spin-conserving hopping—hence  $\lambda < (\delta t)$ —and the pairing gap to be much smaller than the bandwidth—hence  $|\Delta| \ll t$ ; note that for  $|\Delta| \lesssim |\Delta'|$ , we have  $\int d\xi d\xi' / E_p E_s (E_p + E_s) \sim 1/|\Delta'|$  for the integral of Eq. (B3).

We note that the condition for the bulk-to-bulk Josephson coupling to be negligible is different in the higher dimensions  $D = 2, 3$ . This is because, while the maximum gap of the surface term  $|M|$  has the same dependence on the hopping between the two superconductors, the Josephson coupling through the surface term in  $D > 1$  is quadratic rather than linear in the gap of the Majorana surface state. Consequently, when we evaluate Eqs. (10) and (11) of the main text for  $D = 2, 3$ , we obtain the Josephson coupling per site of

$$\frac{1}{N^{D-1}} \frac{\Phi_0 I_c}{2\pi} = \frac{1}{16} \left( \frac{2a}{\pi v |\Delta|} \right)^{D-1} \frac{|M|^2}{|\Delta|} \sim \frac{(\delta t)^4}{t^2 |\Delta|}; \quad (\text{B5})$$

note that the surface-state velocity  $v$ , as it comes from the pairing, is on the order of  $|\Delta|/a$ . On the other hand,

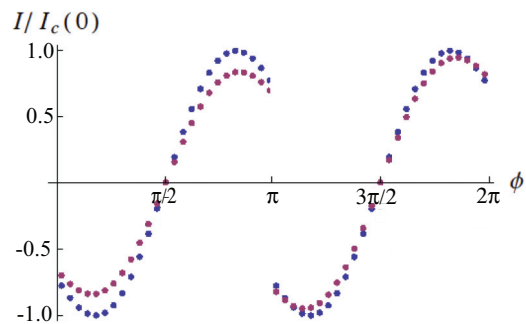


FIG. 4. (Color online) Plot of the Josephson current in  $D = 2$  with the spin-conserving hopping of  $|\delta t/\Delta| = 0.7$  and the spin-flip hopping of  $|\lambda/\delta t| = 0$  (blue dots) and  $|\lambda/\delta t| = 0.2$ .

bulk-to-bulk Josephson coupling would not have a strong dependence on  $D$ , and the ordinary Josephson coupling due to the spin-orbit-coupled hopping across the junction, which would be  $H_{\text{SOC}} = \sum_{n\sigma} \sum_{s=\pm 1} \lambda [\sigma c_{\sigma}^{\dagger}(1, n) f_{\bar{\sigma}}(m, n + s) + \text{H.c.}]$  in  $D = 2$  for example, is of the same order of magnitude per site as that in  $D = 1$ . This means that for  $D > 1$  the conventional Josephson coupling will be much smaller than the Josephson coupling through the Majorana surface state in the limit of

$$|\lambda/\delta t| \ll |\delta t/\Delta|^2; \quad (\text{B6})$$

this is consistent with the singlet-triplet Josephson junction studied by Asano *et al.*<sup>35</sup> We have numerically studied the interplay between topological and regular Josephson effects with the spin-orbit-coupling strength set at  $\lambda/|\Delta| = 0.2$ , which surely overestimates  $\lambda$ , with all the other parameters set the same as for Fig. 3(a) of the main text and, as shown in Fig. 4, we found the first harmonics to be less than 20% of the second harmonics, even though  $|\lambda/\delta t|$  and  $|\delta t/\Delta|^2$  are of the same order of magnitude with our parameters.

<sup>1</sup>X.-L. Qi and S.-C. Zhang, *Rev. Mod. Phys.* **83**, 1057 (2011).

<sup>2</sup>M. Z. Hasan and C. L. Kane, *Rev. Mod. Phys.* **82**, 3045 (2010).

<sup>3</sup>J. E. Moore, *Nature (London)* **464**, 194 (2010).

<sup>4</sup>N. Read and D. Green, *Phys. Rev. B* **61**, 10267 (2000).

<sup>5</sup>A. P. Schnyder, S. Ryu, A. Furusaki, and A. W. W. Ludwig, *Phys. Rev. B* **78**, 195125 (2008).

<sup>6</sup>R. Roy, *arXiv:cond-mat/0608064*; *arXiv:0803.2868*.

<sup>7</sup>X.-L. Qi, T. L. Hughes, S. Raghu, and S.-C. Zhang, *Phys. Rev. Lett.* **102**, 187001 (2009).

<sup>8</sup>S. B. Chung and S. C. Zhang, *Phys. Rev. Lett.* **103**, 235301 (2009).

<sup>9</sup>L. Fu and E. Berg, *Phys. Rev. Lett.* **105**, 097001 (2010).

<sup>10</sup>T. H. Hsieh and L. Fu, *Phys. Rev. Lett.* **108**, 107005 (2012).

<sup>11</sup>S. Sasaki, M. Kriener, K. Segawa, K. Yada, Y. Tanaka, M. Sato, and Y. Ando, *Phys. Rev. Lett.* **107**, 217001 (2011).

<sup>12</sup>B. Yan, C.-X. Liu, H. Zhang, C. Y. Yam, X. L. Qi, T. Frauenheim, and S. C. Zhang, *Europhys. Lett.* **90**, 37002 (2010).

<sup>13</sup>Z. Wang, X.-L. Qi, and S.-C. Zhang, *Phys. Rev. B* **84**, 014527 (2011).

<sup>14</sup>S. Ryu, J. E. Moore, and A. W. W. Ludwig, *Phys. Rev. B* **85**, 045104 (2012).

<sup>15</sup>X.-L. Qi, E. Witten, and S.-C. Zhang, *Phys. Rev. B* **87**, 134519 (2013).

<sup>16</sup>B. Béri, *Phys. Rev. B* **85**, 140501 (2012).

<sup>17</sup>A. J. Niemi and G. W. Semenoff, *Phys. Rev. Lett.* **51**, 2077 (1983).

<sup>18</sup>A. N. Redlich, *Phys. Rev. D* **29**, 2366 (1984).

<sup>19</sup>X.-L. Qi, T. L. Hughes, and S.-C. Zhang, *Phys. Rev. B* **78**, 195424 (2008).

<sup>20</sup>A. Y. Kitaev, *Phys. Usp.* **44**, 131 (2001).

<sup>21</sup>L. Fu and C. L. Kane, *Phys. Rev. Lett.* **100**, 096407 (2008).

<sup>22</sup>I. J. Lee, M. J. Naughton, G. M. Danner, and P. M. Chaikin, *Phys. Rev. Lett.* **78**, 3555 (1997).

<sup>23</sup>J.-F. Mercure, A. F. Bangura, X. Xu, N. Wakeham, A. Carrington, P. Walmsley, M. Greenblatt, and N. E. Hussey, *Phys. Rev. Lett.* **108**, 187003 (2012).

<sup>24</sup>F. S. Nogueira and I. Eremin, *J. Phys.: Condens. Matter* **24**, 325701 (2012).

- <sup>25</sup>Y. Niu, S. B. Chung, C.-H. Hsu, I. Mandal, S. Raghu, and S. Chakravarty, *Phys. Rev. B* **85**, 035110 (2012).
- <sup>26</sup>A. Zazunov and R. Egger, *Phys. Rev. B* **85**, 104514 (2012).
- <sup>27</sup>M. Fogelström and S.-K. Yip, *Phys. Rev. B* **57**, R14060 (1998); M. Fogelström, D. Rainer, and J. A. Sauls, *Phys. Rev. Lett.* **79**, 281 (1997).
- <sup>28</sup>H.-J. Kwon, K. Sengupta, and V. M. Yakovenko, *Eur. Phys. J. B* **37**, 349 (2004); K. Sengupta, and V. M. Yakovenko, *Phys. Rev. Lett.* **101**, 187003 (2008).
- <sup>29</sup>A. I. Buzdin, L. N. Bulaevskii, and S. Panjukov, *Pis'ma Zh. Eksp. Teor. Fiz.* **35**, 147 (1982) [*JETP Lett.* **35**, 178 (1982)].
- <sup>30</sup>B. van Heck, F. Hassler, A. R. Akhmerov, and C. W. J. Beenakker, *Phys. Rev. B* **84**, 180502 (2011).
- <sup>31</sup>L. Fu and C. L. Kane, *Phys. Rev. B* **79**, 161408 (2009).
- <sup>32</sup>R. Shindou, A. Furusaki, and N. Nagaosa, *Phys. Rev. B* **82**, 180505 (2010).
- <sup>33</sup>C.-K. Lu and S. Yip, *Phys. Rev. B* **80**, 024504 (2009); Z. Yang, J. Wang, and K. S. Chan, *J. Phys.: Condens. Matter* **23**, 085701 (2011).
- <sup>34</sup>L. I. Glazman and M. E. Raikh, *Pis'ma Zh. Eksp. Teor. Fiz.* **47**, 378 (1988) [*JETP Lett.* **47**, 452 (1988)].
- <sup>35</sup>Y. Asano, Y. Tanaka, M. Sigrist, and S. Kashiwaya, *Phys. Rev. B* **67**, 184505 (2003).